Peptide-Carbazolyl Cyanobenzene Conjugates: Enabling Biomolecule Functionalization via Photoredox and Energy Transfer Catalysis

Xing-Yu Liu[1], Wei Cai[2], Anne-Sophie Chauvin[3], Beat Fierz[2], Jerome Waser*[1]

Abstract: Since their discovery in 2012, carbazolyl (iso)phthalonitrile derivatives (Cz(I)PN) have found significant applications in organic light emitting diodes (OLEDs) and as photocatalysts in organic chemistry. Herein, we introduce two efficient methods for incorporating carbazolyl cyanobenzenes into various peptide sequences. The first method involves a photomediated decarboxylative functionalization of the C-terminus of peptides, leading to the formation of various carbazolyl benzonitrile (CzBN) derivatives. The second method exploits a cysteine-selective S_NAr reaction on a fluorinated arene precursor, resulting in novel peptide-3CzIPN (Triscarbazolyl-isophthalonitrile) conjugates. Both types of conjugates maintain delayed fluorescence properties, exhibit similar or wider redox potential, and possess higher excited state energy when compared to currently used cyanoarenes. We demonstrated the photocatalytic activity of these conjugates first through a photo-mediated peptide C-terminal decarboxylative alkynylation. Then, water-soluble peptide conjugates were used to catalyze a thiol-ene reaction on cysteine in aqueous media. Finally, we achieved protein labeling via aryl azide excitation both in vitro and at the cellular level using peptide-CzIPN conjugates. By incorporating a peptide ligand of the protein integrin $\alpha_v\beta_3$, proximity-labeling next to this target was realized by aryl azide excitation in living cells, showing an excellent overlap with antibody-based imaging. These findings reveal the potential of cyanoarene-peptide conjugates for proximity-driven photochemistry in complex biological systems.

Visible-light-mediated biomolecule functionalization has emerged as a powerful tool for achieving spatiotemporal control of reactions within complex biological systems.[1,2,3,4,5] Compared to traditional UV-induced transformations, the combination of visible light and photocatalysts enables the generation of highly reactive intermediates under milder conditions in close proximity to the excited photocatalysts. The photocatalyst can then be localized in a desired site on a biomolecule using a binding small molecule,[6,7,8] a peptide[9] or a protein/antibody.[4] To facilitate site-specific functionalization in intricate and highly diluted biological environments, photocatalysts have been designed with a wide redox potential window for single-electron transfer (SET) and a long-lived, high-energy excited state for efficient energy transfer (EnT). However, these catalysts are often transition metal complexes, for example iridium (Ir) and ruthenium (Ru) complexes, which are potentially cytotoxic to living systems.[10,11] In contrast, the use of non-toxic organic photosensitizers is much less exploited. Recent studies have demonstrated the potential of organic dyes, including rhodamine,[12] fluorescein,[13] and flavin,[14] in enabling biomolecule functionalization in living

[1]Laboratory of Catalysis and Organic Synthesis (LCSO), École Polytechnique Fédérale de Lausanne, EPFL, 1015 Lausanne, Switzerland
[2] Laboratory of Biophysical Chemistry of Macromolecules (LCBM), Ecole Polytechnique Fédérale de Lausanne, EPFL, 1015 Lausanne, Switzerland
[3] Group of Coordination Chemistry, Institut des Sciences et Ingénierie Chimiques, École Polytechnique Fédérale de Lausanne, EPFL, 1015 Lausanne, Switzerland

systems through visible light excitation. Given the excellent biocompatibility of organic photosensitizers, these recent pioneering breakthroughs are promising and demonstrate the urgent need for novel organic dyes with unique photophysical properties and improved biocompatibility.

Carbazolyl (iso)phthalonitrile (Cz(I)PN) derivatives are a class of organic dyes with carbazoles as electron donors and a dicyanobenzene as an electron acceptor (Figure 1a).[15] The small energy gap between the singlet and triplet excited states of these compounds enhances reversible intersystem crossing (RISC), making them suitable for use in organic light-emitting diodes (OLEDs) with thermally activated delayed fluorescence (TADF). Excellent quantum yield (up to 94.6%), a long-excited state lifetime (up to 5.1 μs) and a wide redox potential window make them also good photocatalysts in different light-driven transformations.[16,17,18,19,20] Additionally, the fine-tuning of the photocatalysts can be easily realized by adding electron-withdrawing and electron-donating groups on the carbazole motifs. Since the seminal discovery by Zhang in 2016,[21] over 20 structural variants of CzIPN have been investigated for their photocatalytic properties. These derivatives have shown potential not only as substitutes for traditional iridium (Ir) and ruthenium (Ru) catalysts, but also have enabled novel transformations for photo-mediated small molecule functionalization.

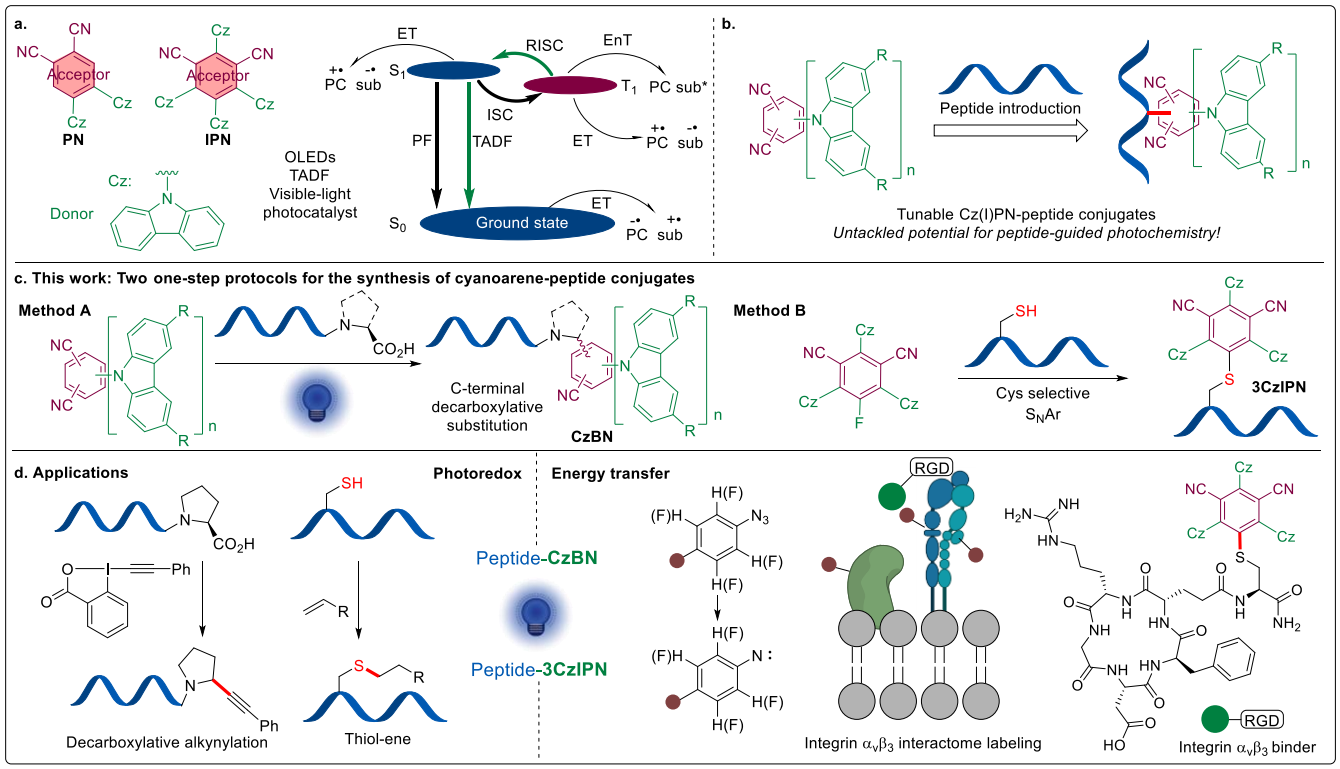

Figure 1. a. Structure of carbazolyl (iso)phthalonitrile (Cz(I)PN) derivatives and energy diagram for their use as photocatalysts (PC) in ET (electron transfer) and EnT (energy transfer) based transformations. b. Peptide-Cz(I)PN-conjugates: unprecedented hybrid catalysts for peptide-directed photochemistry. c) Synthesis of CzBN-peptide conjugates via decarboxylative arylation at peptide C-terminus (**method A**) and 3CzIPN-peptide conjugates via S_NAr on cysteine (**method B**). d. Application to biomolecule functionalization.

Despite the extensive use of Cz(I)PN derivatives in single-electron transfer (SET) and energy transfer (EnT) catalysis for small molecule functionalization, their applications in biological contexts have been limited.[22] The incorporation of peptide sequences interacting with biological targets would enable the use of Cz(I)PN for proximity-driven reactions, with the added advantage of increasing their water solubility (Figure 1b). Surprisingly, such a strategy has not been reported yet.

Herein, we describe two efficient one-step approaches to synthesize cyanoarenes bearing functional peptide sequences (Figure 1c). The first method (**Method A**) involves the photo-mediated decarboxylative substitution of a cyanide group in Cz(I)PN. A broad scope of carbazolyl benzonitriles (CzBN) was obtained, but the reaction resulted in the formation of diastereoisomers at the newly formed benzylic center at C-terminus. To further enhance the incorporation efficiency and prevent the generation of two diastereoisomers, we developed a cysteine-selective S_NAr reaction using a fluoroisophthalonitrile precursor resulting in the formation of a triscarbazolyl-isophthalonitrile (3CzIPN) dye (**Method B**). Both the CzBN and the 3CzIPN conjugates exhibit photophysical properties and redox potentials that are similar to or superior to the non-modified 4CzIPN. These properties make them suitable as photocatalysts in various photo-mediated biomolecule functionalizations, both in vitro and at the cellular level. We demonstrated first successful decarboxylative alkynylation and thiol-ene reactions on peptides. As a first example in a complex biological setting, we then realized a proximity-driven labelling next to integrin $\alpha_v\beta_3$ via aryl azide excitation enabled by a binding peptide-CzIPN conjugate, which showed an excellent overlap with antibody-based imaging.

Results

In 2019, König's group reported a general decarboxylative photosubstitution of dicyanobenzene-based photocatalysts under blue light irradiation.[23,24] The alkyl radical, generated through decarboxylation, can be trapped by the radical anion formed after reduction of the photocatalyst. The substituted products are formed after a subsequent cyanide elimination. The monocyanobenzene products are still blue TADF emitters and reducing photocatalysts.[25,26] However, amino acids or peptides have not been used as carboxylic acid partners in this transformation. During our studies on the decarboxylative alkynylation of peptide C-termini,[27,28] we also observed decarboxylative photosubstitution products between amino acids/peptides and 4CzIPN, which motivated us to optimize this transformation. Gratifyingly, the radical substitution could be achieved by simply shedding blue light on a mixture of peptide, 4CzIPN and K_2CO_3 for model substrate **3aa** (see Table S1 in Supporting Information for reaction optimization). To assess the generality of our method, we first investigated systematically different amino acids on smaller tetrapeptides bearing a Pro at the C-terminus, which has been reported to be the most efficient amino acid for decarboxylative functionalization[27] (Figure 2, **3aa**-**3pa**). Arg (**3ba**), Met (**3ca**), Asp (**3da**), amides (**3ea**, **3fa**), Lys (**3ga**), alcohols (**3ha**, **3ia**), a terminal alkyne (**3ja**) as well as Tyr (**3pa**) were all tolerated, resulting in 24-81% yield of the corresponding products. Trp (**3ka**) was not compatible with the photoredox conditions due to its susceptibility to oxidation. We then expanded our investigation to different C-terminal amino acids (products **3la**-**3oa**). Glu and pipecolic acid could be converted to the desired decarboxylation products **3ma** and **3oa** in 20% and 46% yield,

under the same reaction conditions. For Ala (**3la**) and Phe (**3na**), it was necessary to use a stronger 440 nm Kessil lamp. This modification significantly improved the conversion of peptides, although it also led to more degradation of 4CzIPN.

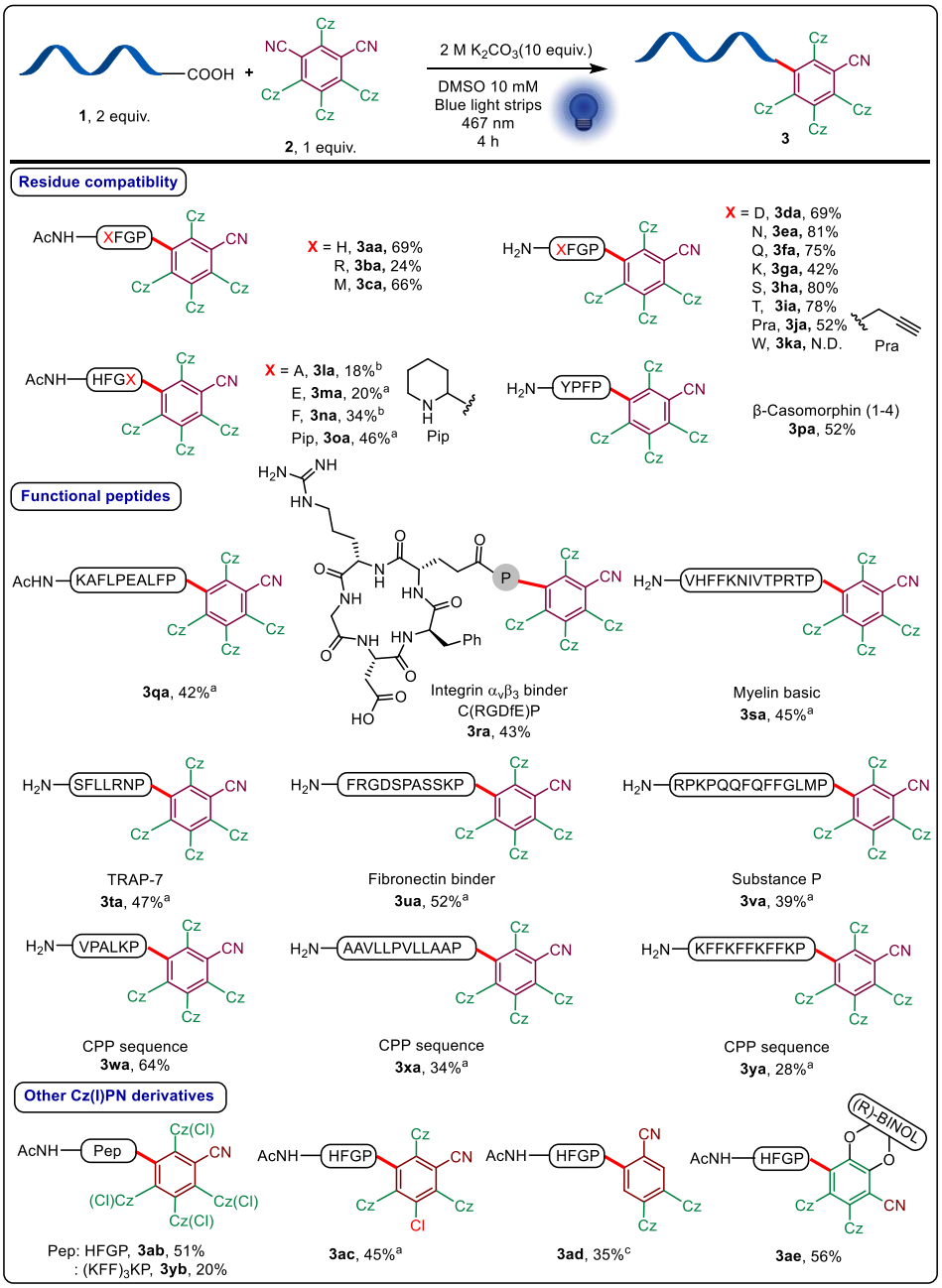

Figure 2. Scope of the C-terminal decarboxylative substitution, the d.r. of the product was not determined. The reactions were performed on a 0.01 mmol scale, isolated yields are provided. Cz(Cl): 3,6-dichlorocarbazoyl. (R)-BINOL: (R)-1,1′-Bi-2-naphthol. [a]The reactions were conducted overnight. [b]A 440 nm Kessil lamp (40 W, intensity: 25%) was used as the blue LED source for 1 hour. [c] A 390 nm Kessil lamp (40 W, intensity: 25%) was used as the light source for 2 hours.

Encouraged by the excellent functional group tolerance and chemoselectivity of the transformation, we applied it to more complex peptides (Figure 2, **3pa**-**3ya**). β-casomorphin (1-4),[29] containing a free Tyr and N-terminus, was transformed into conjugate **3pa** in 52% yield. Decamer **1q**, with a free Glu residue, was selectively functionalized at the C-terminus, yielding

3qa exclusively. Other successfully modified bioactive peptides include an $\alpha_v\beta_3$ integrin binding cyclic peptide (**3ra)**,[30] myelin basic protein fragment 87-99 (**3sa**), which induces T cell proliferation,[31] TRAP-7 (**3ta)**, a thrombin receptor activator, [32] a fibronectin binding inhibitor (**3ua**)[33] and the neurotransmitter substance P (**3va**). We also synthesized conjugates **3wa-3ya** starting from three cell-penetrating peptide sequences (VPALK,[34] AAVLLPVLLAA[35] and $(KFF)_3K$[36]) with different length and hydrophilicity with added Pro at C terminus to facilitate reaction with 4CzIPN. Finally, we extended this reaction to other Cz(I)PN derivatives. 4ClCzIPN (**2b**) and 3CzClIPN[37] (**2c**) were converted to products **3ab, 3yb** and **3ac** in 20-51% yield. Although 2CzPN (**2d**) exhibited lower reactivity due to weak absorption under blue light irradiation, the yield significantly improved upon switching the light source from 467 nm strips to a 390 nm Kessil lamp. Additionally, a chiral BINOL-derivative **2e**, known as a TADF emitter for circularly polarized light emission,[38] yielded conjugate **3ae** in 56% yield.

Overall, the method could be applied to a large scope of peptides and Cz(I)PN derivatives. Nevertheless, the moderate incorporation efficiency for longer peptide sequences, the need for excess amounts of peptides, and the generation of 1:1 diastereomeric mixtures in most cases can be a drawback for certain applications. Inspired by the reported synthesis of 4CzIPN derivatives via an S_NAr reaction of different carbazoles on 3CzFIPN (**5**),[39] we attempted to use Cys as a nucleophile in this transformation (Figure 3). To our delight, the S_NAr reaction could be achieved in an open flask with DMSO and a Tris buffer as reaction solvents (see Table S2 in the Supporting Information for reaction optimization). From the amino acid cysteine to pentameric peptides, the introduction of 3CzIPN occurred in 67-88% yield with exclusive formation of the desired products **6aa-6ea**. Cys within a cationic cell penetrating peptide TAT[40] can also be selectively modified, affording **6fa**. Additionally, 3CzIPN was successfully introduced onto a mitochondria localization sequence (MLS)[41] and a nucleus localization sequence (NLS)[42] to give **6ga** and **6ha**. In the case of cyclic peptide **5l**, a potent $\alpha_v\beta_3$ integrin binder, Cys at the C-terminus was selectively modified leading to **6ia** in 65% yield. Furthermore, Substance P yielded peptide conjugate **6ka**. Two α-helical peptides binding to the protein β-catenin[43] and MDM2[44] gave conjugates **6na** and **6ma**, respectively.

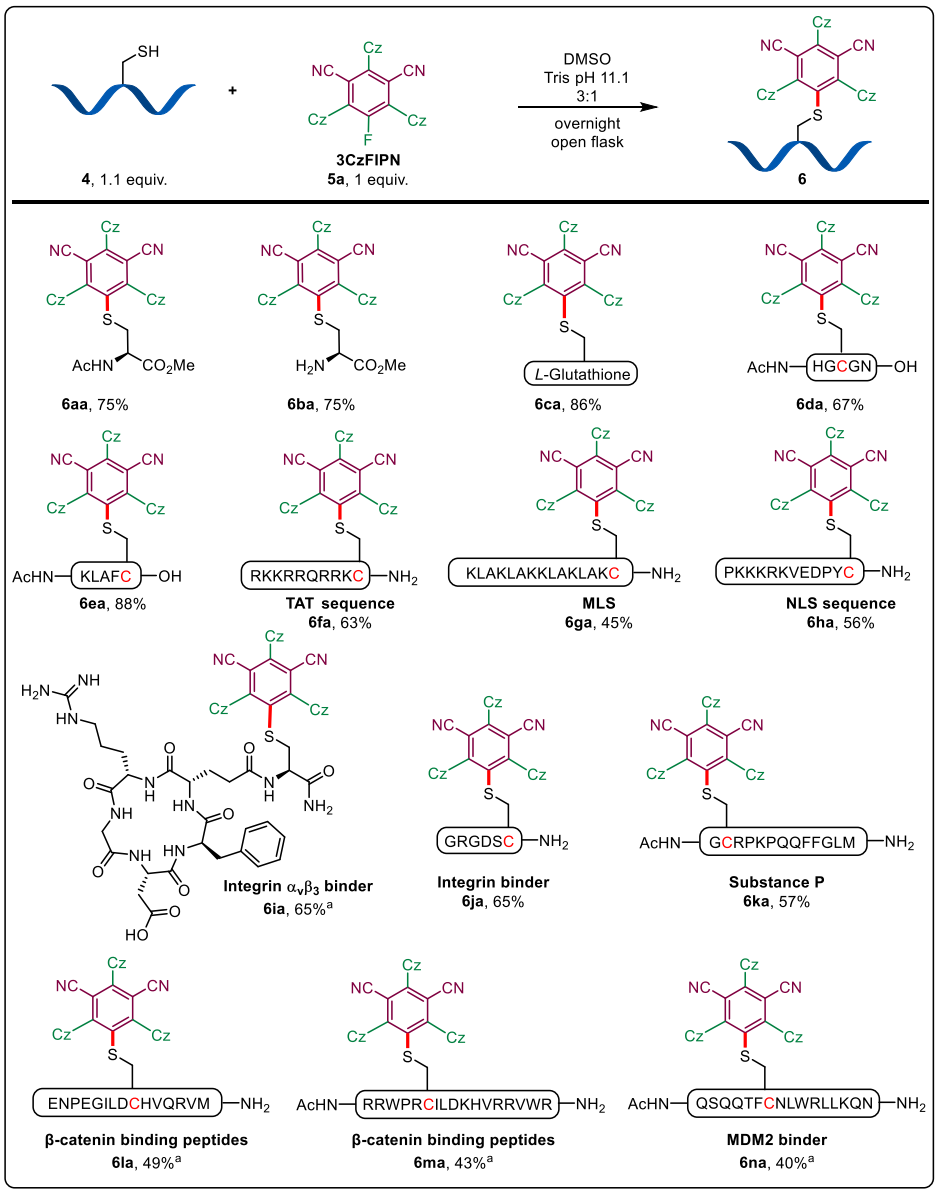

Figure 3. Scope of Cys-selective S_NAr. The reactions were performed on a 0.01 mmol scale, isolated yields are given. [a] 1.0 equiv. of peptide and 1.1 equiv. of 3CzFIPN were used.

With various Cz(I)PN-peptide conjugates in hand, we determined their photophysical properties to evaluate their potential as biocompatible photocatalysts. The absorption spectra feature several bands located below 400 nm, which are attributed to the donor-acceptor $\pi \rightarrow \pi^*$ transition of the carbazole-cyanobenzene.[45] An additional band extending to 450 nm is observed for all 3/4 carbazolyl conjugates, in DMSO or in water, matching with the excitation spectra (Figure 4 and Figure S1 in Supporting Information). In DMSO, the excitation spectra of 4CzlPN and its peptide conjugates show three distinct peaks at 290, 318, and 330 nm, along with a broad band extending up to 350 nm. The spectra of 8Cl-4CzlPN and its conjugates are blue-shifted by approximately 1150–1450 cm^{-1} (Figure 4). Additionally, the emission maximum of 8Cl-4CzlPN is blue-shifted by around 334 cm^{-1} compared to 4CzlPN. The emission of **6ca** is only slightly shifted (368 cm^{-1}) compared to its parent dye 4CzlPN, while **3ya** shows a more pronounced blue shift of 1884 cm^{-1}. Similarly, the shift observed between **3yb** and 8Cl-4CzlPN is 1833 cm^{-1}. A slight red shift was noted for the **3yb** and **6ca** conjugates

when the solvent was changed from DMSO to water (Figure S2 in Supporting Information), likely due to intramolecular charge transfer (ICT) influenced by the hydrophobic Cz(I)PN cores. [46] Water, known to quench luminescence due to competition with non-radiative deactivation pathways, caused a decrease in both emission and excitation intensities, although they remained relatively strong. The lifetimes of the different compounds were studied at 330 nm and 380 nm to broaden applicability for biological studies.

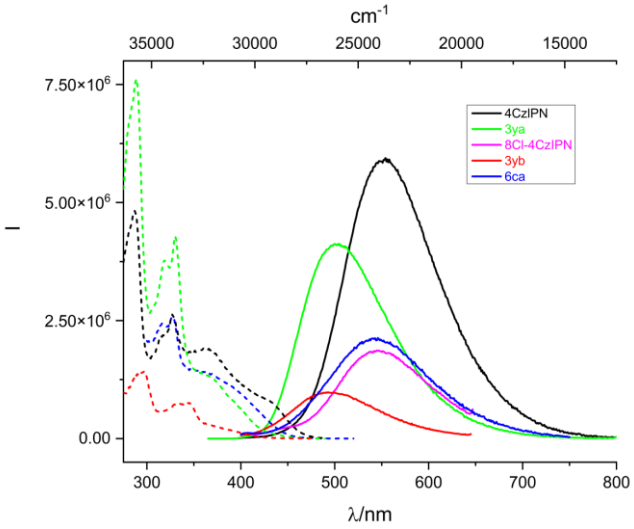

Figure 4. Corrected excitation and emission spectra of the different CzPN-peptide conjugates at room temperature, in DMSO (10 μM). Solid lines: emission spectra with λ_{ex}= 330 nm Dashed lines: excitation spectra, λ_{em} corresponds to the maximum of the emission spectra, see table S3 for exact values.

The results (Table S2 in Supporting Information) showed that decay curves fit best with a double exponential model. The first decay was minimally affected compared to the unsubstituted dyes (0.99-1.72 vs 1.52 μs for 4CzIPN and its derivatives), while the second was shorter (8.60-8.81 vs 11.6 μs for 4CzIPN and its derivatives). The conjugate lifetimes were consistent across different solvents and peptide conjugations. Notably, in water, **3yb** showed increased lifetimes, suggesting small aggregate formation. In DMSO, the quantum yield of unmodified 4CzIPN is 19.7% under excitation at 330 nm (Table S3, S4 in Supporting Information), aligning with the 10% yield previously reported in aerated toluene.[11] The quantum yield of **3ya** in DMSO remained close, while other peptide conjugates showed yields around 7-8%. Under 380 nm excitation, quantum yields were slightly lower. Notably, these compounds still exhibited good quantum yields in water, providing potential for biological applications.

To further compare the redox potentials and excited-state energy of the peptide conjugates with unmodified 4CzIPN and a well-known Ir complex $[Ir\{dF(CF_3)ppy\}_2(dtbpy)]PF_6$, Cyclic voltammetry (CV) experiments were conducted (Figure 5, Table S5 in Supporting Information), and excited state potentials were estimated using the Rehm-Weller equation. In the excited states, both conjugates exhibit similar or even stronger oxidative and reductive capabilities when compared to 4CzIPN and the Ir catalysts. They also possess high excited states energy (>60 kcal/mol), with **3za** notably reaching 67.6 kcal/mol.[24]

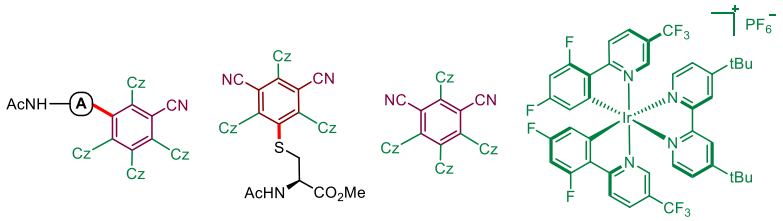

	3za	6aa	4CzIPN	[Ir{dF(CF$_3$)ppy}$_2$(dtbpy)]PF$_6$
$E_{1/2}(P^*/P^-)$ V	+1.34	+1.24	+1.35	+1.21
$E_{1/2}(P^+/P^*)$ V	-1.50	-1.01	-1.04	-0.89
$E_{0\text{-}0}$ V (kcal/mol)	2.93(67.6)	2.65(61.1)	2.56(59.0)	2.61(60.1)

Figure 5. Structure and redox potentials of CzBN and CzIPN-peptide conjugates. 4CzIPN and Ir photocatalyst are shown as comparison. See Supporting information for a full list of redox values (Table S5).

The broader redox-potential window, long excited state lifetimes, higher excited state energy, and enhanced solubility of CzBN and CzIPN derivatives in aqueous media indicated a high potential for the photo-functionalization of biomolecules. First, we attempted the photo-mediated C-terminal decarboxylative alkynylation of peptides originally catalyzed by 4CzIPN (Figure 6a). Compared to 4CzIPN, conjugates **3za** and **6aa** produced the alkynylated product **8a** with a slight decrease of yield for the protected dipeptide Cbz-GP-OH. We further tested the catalytic reactivity of the conjugates on a longer tetramer peptide, AcHFGP-OH. The alkynylation reaction (**8b**) proceeded with both conjugates **3za** and **6aa**, achieving HPLC yields of 15% and 51%, respectively. The latter is comparable to the yield obtained with non-modified 4CzIPN (52%). Encouraged by these results, we conducted this reaction in aqueous media using water-soluble conjugates **3ya** and **6ca**. Unfortunately, no decarboxylation occurred with either catalyst using a simple dipeptide as the model substrate, likely due to differences in redox potential for the dyes in the two reaction solvents.

We next explored the feasibility of conducting a visible light-mediated thiol-ene reaction in aqueous media using CzBN and CzIPN conjugates as photocatalysts (Figure 6b). To date, there are only a few examples of thiol-ene reactions carried out in aqueous media under visible light excitation.[47,48] Employing similar conditions to those reported previously, we were pleased to find that the desired thiol-ene adduct could be efficiently synthesized from Ac-Cys-OH and allyl alcohol in aqueous media, using conjugates **3ya** and **6ca** as photocatalysts. In contrast, 4CzIPN exhibited significantly lower catalytic reactivity due to its limited solubility in water. We further examined the compatibility of this reaction with longer peptide sequences. Conjugate **6ca** demonstrated superior catalytic activity compared to **3ya**, as the latter led to increased oxidation of the peptides during the photocatalytic process. Consequently, **6ca** was selected as the preferred photocatalyst for thiol-ene reactions involving longer peptides. This reaction showed good tolerance for a variety of unprotected side-chain residues, yielding the desired thiol-ene adduct **10b** with high efficiency. Moreover, the reaction was not limited to allyl alcohol **9a**; a biotin-containing alkene **9b** can also be incorporated into peptides, yielding the thiol-ene product **10c** and **10d**.

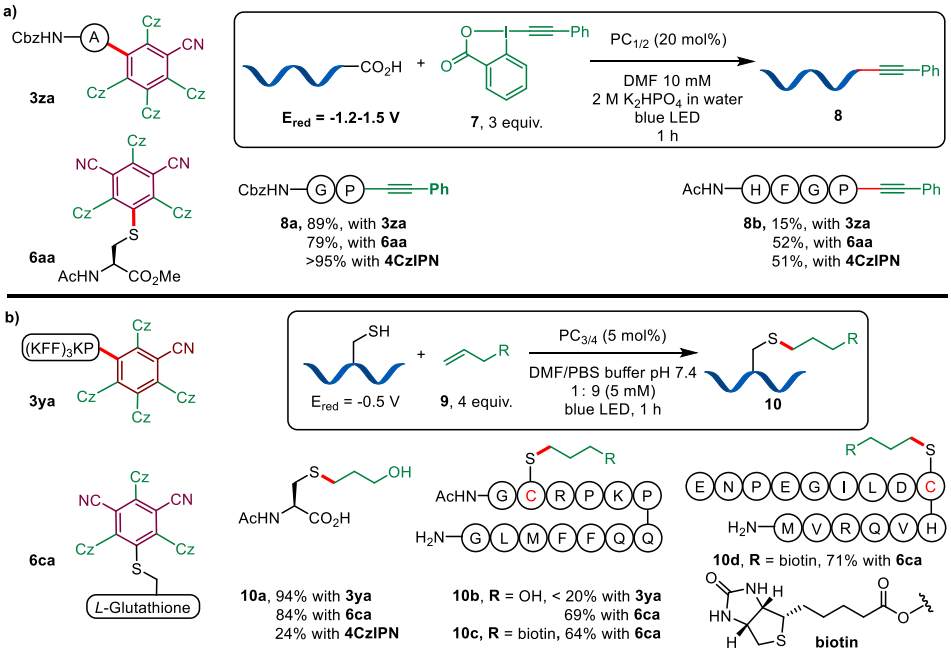

Figure 6. Application of CzBN- and CzIPN-peptide conjugates in the photo-mediated decarboxylative alkynylation and the thiol-ene reactions. Yields were determined based on the integration of HPLC-UV signals.

Then, we aimed to determine whether aryl azides **11**, with a triplet state energy of 43.9 kcal/mol, could be excited through energy transfer (EnT) using the peptide conjugates (excited energy above 60.0 kcal/mol).[8,49,50,51] We were pleased to observe successful excitation of both aryl azide and perfluorinated aryl azide using either 4CzBN **3za** or 3CzIPN conjugates **6aa** under 467 nm irradiation from a Kessil lamp (See Supporting Information section 8.3.2 for details). Notably, 3CzIPN conjugates exhibited higher excitation efficiency. Encouraged by these results, we further explored the potential of in-vitro protein labelling enabled by these dye conjugates (Figure 7a). We conducted the reaction on bovine serum albumin (BSA) using a biotin-conjugated aryl azide probe (**11a**) with a PEG linker to enhance water solubility. The photolabeling reactivity of the conjugates was assessed via Western blotting of the reaction mixture with HRP-conjugated streptavidin to detect the amount of biotinylated BSA. A notable biotinylation level was observed when the reaction was performed in a PBS buffer after only 15 minutes of irradiation with a 467 nm Kessil lamp (40 W, intensity: 100%) in the presence of **6ca**. The level of protein biotinylation correlated with the concentration of **6ca**. In contrast, direct excitation of BSA with 467 nm light alone resulted in minimal labelling. Similar outcomes were observed with perfluorinated aryl azide excitation (**11b**), a compound that facilitates the generation of nitrene species with extended lifetimes, providing protein labelling with different labelling radius.[49]

With the success of in-vitro protein labelling via aryl azide excitation, we extended this method to living cell systems with the goal to exploit the potential for proximity-driven labelling offered by the binding peptide. Compared to the previous aryl azide excitation with a Ir and Os catalyst, which required the pre-installation of photocatalyst onto an antibody, and was limited to extracellular protein targets,[4,49-51] peptide sequences allow us potentially to target both intra- and extracellular targets. To validate the potential of targeting intracellular targets, we used

CPP (cell penetrating peptide)-3CzIPN conjugate **6fa** as the photosensitizer together with azide **11c**, which is small enough to cross the cell membrane (Figure 7b, DIC imaging in Supporting Information Section 8.7.2). We observed significant fluorescent pattern overlap between the nitrene labelling region (revealed through CuAAC between a Cy5 azide reagent and the terminal alkyne on **11c**) and the CzIPN conjugate region inside Hela cells (See Supporting Information section 8.7 for experimental details).

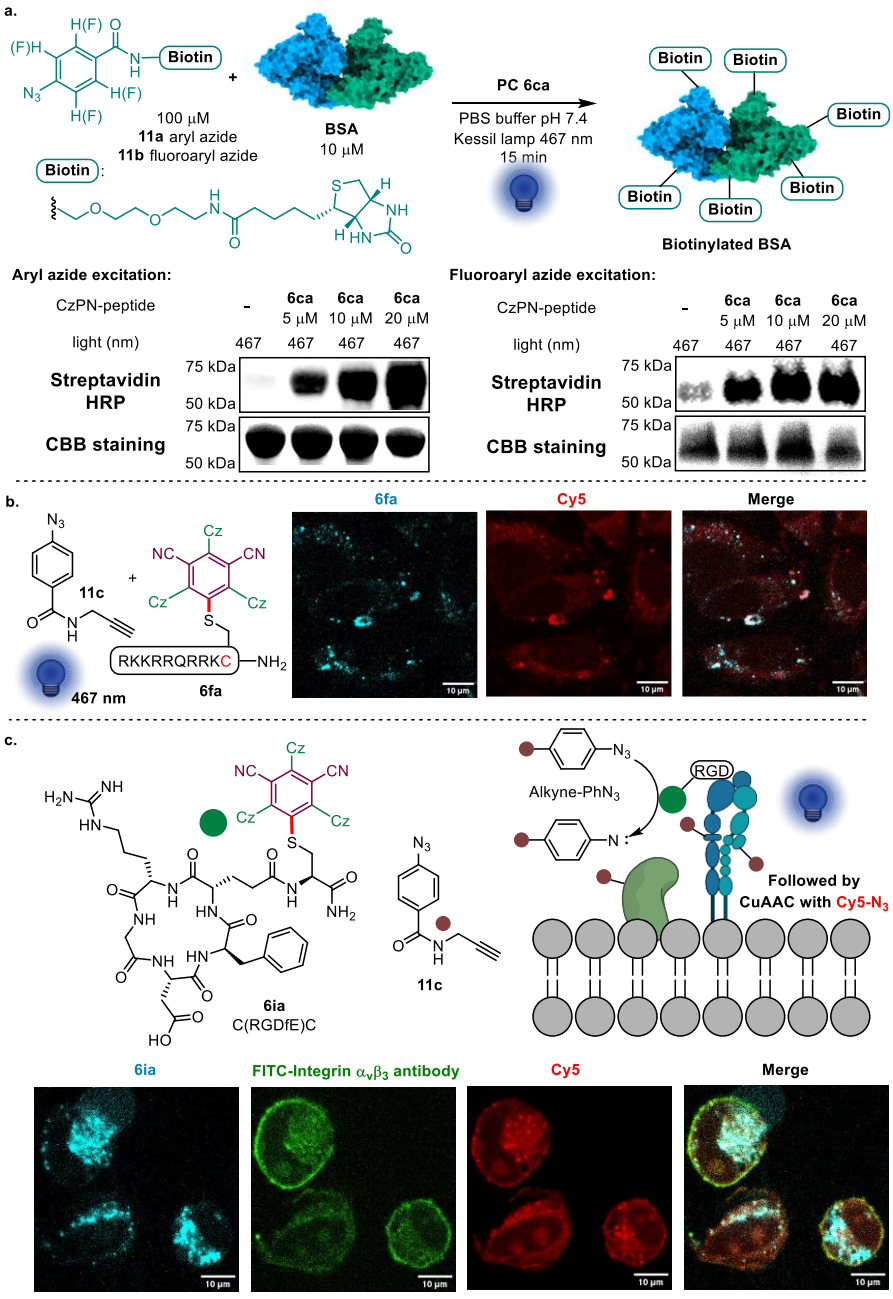

Figure 7. Aryl azide excitation for in vitro and cellular protein labelling. Kessil lamp 467 nm (40 W, intensity: 100%) was used as the light source. a. Protein labelling in vitro via aryl azide excitation using CzPN-peptide conjugate **6ca**. b. Labelling using cell-penetrating 3CzIPN conjugate **6fa** via nitrene formation. Cell line: Hela. DIC imaging in Supporting information Section 8.7.2. c. Peptide-guided proximity labelling of integrin $\alpha_v\beta_3$ with conjugate **6ia** (10 μM) via nitrene formation followed by immunofluorescence analysis using FITC-integrin $\alpha_v\beta_3$ monoclonal antibody to confirm target specific labelling. Cell line: A549. DIC imaging in Supporting information Section 8.7.3.Scale bar: 10 μm. For

quantitative image analysis, the following threshold were used: FITC-integrin $\alpha_v\beta_3$ monoclonal antibody channel: 741. Cy5 channel: 109. Pearson's coefficient for FITC-integrin $\alpha_v\beta_3$ monoclonal antibody and Cy5: 0.628.

As an extracellular target of high biological relevance, we chose integrins, which are a class of cell adhesion receptors playing a crucial role in mediating signal transduction between cells and the extracellular matrix (ECM). Notably, the αvβ3 integrin subtype is frequently overexpressed in different cancer cells. Consequently, it has emerged as a promising therapeutic target for the development of cancer treatments.[52,53] To further underscore the application of peptide sequences on 3CzIPN to realize protein specific labelling, we used the modified integrin αvβ3 binder **6ia** to probe the interactome of integrin αvβ3 (Figure 7c, DIC imaging in Supporting Information Section 8.7.3). We selected the A549 cell line, known for its high expression of integrin αvβ3. The cells were first incubated with the integrin αvβ3 binder **6ia** for one hour, followed by washing and subsequent incubation with the aryl azide probe **11c**. After the photoexcitation of aryl azide probe, the cells were fixed and subjected to immunofluorescence (IF) staining with FITC conjugated integrin αvβ3 antibody to determine the localization of the target protein. The labeling region of the aryl azide was visualized through CuAAC between a Cy5 azide reagent and the terminal alkyne on **11c**. We were pleased to observe a strong overlap between the antibody signal and the Cy5 signal, showing that aryl azide excitation had occurred in a close proximity to integrin. After the photoreaction, the localization of the photocatalyst **6ia** also showed a good overlap with both the andibody and the Cy5 dye, although the signal on the membrane was weaker. This may be due to a fast photo-bleaching of the dye on the membrane during irradiation. In both the cases of intracellular and extracellular aryl azide excitation, cells remained in good viability before and after light irradiation, highlighting the potential of using 3CzIPN-peptide conjugates in live systems (Figure S5).

Conclusion

We have developed two efficient strategies to incorporate privileged cyanobenzene organic photocatalysts into functional peptides. The first approach involved a photo-mediated, C-terminal selective decarboxylative arylation, enabling the attachment of various peptides to diverse CzBN cores. The second approach leveraged a cysteine-selective S_NAr reaction with 3CzFIPN, which improved reaction efficiency and avoided the issue of diastereoisomer formation at peptide C-termini. The resulting peptide-CzBN and CzIPN conjugates exhibited strong delayed fluorescence, broad redox potential windows, and high excited state energies. We demonstrated the potential of using these conjugates as photocatalyst for biomolecule functionalization through a photo-mediated decarboxylative alkynylation in organic solvents and a thiol-ene reaction in aqueous media. Additionally, the conjugated promoted aryl azide excitation, enabling protein labeling both in vitro and at the cellular level. Using a peptidic ligand of integrin αvβ3, proximity-labeling of the protein and its interactome became possible via aryl azide excitation. We believe these conjugates will open new avenues for the development of novel photo-mediated biomolecule functionalizations in biological contexts.

Author Contributions:

X.L. performed the experiments under the supervision of J.W.. W.C. conducted the western blot and cell experiments under the supervision of B.F.. A.C. conducted the photophysical studies of peptide-CzPN conjugates, including data analysis and draft preparation. X.L and J.W. contributed to the overall design of the study, data analysis and writing of the manuscript.

Acknowledgment:

We would like to acknowledge the European Research Council for financial support (ERC Consolidator GrantSeleCHEM, No. 771170). We thank the MS service from EPFL-ISIC for their support. We thank Mr. Tak Hin Wong from LCS EPFL for his instruction on cyclic voltammetry measurement. We thank Dr. Stefano Nicolai from LCSO EPFL for the preparation of fluroaryl azide probes.

References:

[1] Lechner, V. M. *et al.* Visible-Light-Mediated Modification and Manipulation of Biomacromolecules. *Chem. Rev.* **122**, 1752-1829, (2022).
[2] Ryu, K. A., Kaszuba, C. M., Bissonnette, N. B., Oslund, R. C. & Fadeyi, O. O. Interrogating biological systems using visible-light-powered catalysis. *Nat Rev Chem* **5**, 322-337, (2021).
[3] Liu, Z., Okamoto, Y. & Sato, S. Photocatalytic Structures for Protein Modifications. *ChemCatChem* **16**, e202301424, (2024).
[4] Knutson, S. D., Buksh, B. F., Huth, S. W., Morgan, D. C. & MacMillan, D. W. C. Current advances in photocatalytic proximity labeling. *Cell Chem. Biol.* **31**, 1145-1161, (2024).
[5] Liu, Y. *et al.* Proximity Chemistry in Living Systems. *CCS Chem.* **5**, 802–813 (2023).
[6] Sato, S. & Nakamura, H. Ligand-Directed Selective Protein Modification Based on Local Single-Electron-Transfer Catalysis. *Angew. Chem., Int. Ed.* **52**, 8681–8684 (2013).
[7] Trowbridge, A. D. *et al.* Small molecule photocatalysis enables drug target identification via energy transfer. *Proc. Natl. Acad. Sci. U. S. A* **119**, e2208077119 (2022).
[8] Huth, S. W. *et al.* µMap Photoproximity Labeling Enables Small Molecule Binding Site Mapping. *J. Am. Chem. Soc.* **145**, 16289–16296 (2023).
[9] Seath, C. P. *et al.* Tracking chromatin state changes using nanoscale photo-proximity labelling. *Nature* **616**, 574–580 (2023).
[10] Sletten, E. M. & Bertozzi, C. R. Bioorthogonal Chemistry: Fishing for Selectivity in a Sea of Functionality. *Angew. Chem., Int. Ed.* **48**, 6974-6998, (2009).
[11] Ravelli, D., Fagnoni, M. & Albini, A. Photoorganocatalysis. What for? *Chem. Soc. Rev.* **42**, 97-113, (2013).
[12] Wang, H. *et al.* Selective Mitochondrial Protein Labeling Enabled by Biocompatible Photocatalytic Reactions inside Live Cells. *JACS Au* **1**, 1066-1075, (2021).
[13] Tamura, T., Takato, M., Shiono, K. & Hamachi, I. Development of a Photoactivatable Proximity Labeling Method for the Identification of Nuclear Proteins. *Chem. Lett.* **49**, 145–148 (2020).
[14] Oslund, R. C. *et al.* Detection of cell–cell interactions via photocatalytic cell tagging. *Nat Chem Bio* **18**, 850–858 (2022).
[15] Uoyama, H., Goushi, K., Shizu, K., Nomura, H. & Adachi, C. Highly efficient organic light-emitting diodes from delayed fluorescence. *Nature* **492**, 234-238, (2012).
[16] Bryden, M. A. & Zysman-Colman, E. Organic thermally activated delayed fluorescence (TADF) compounds used in photocatalysis. *Chem. Soc. Rev.* **50**, 7587-7680, (2021).
[17] Shang, T.-Y. *et al.* Recent advances of 1,2,3,5-tetrakis(carbazol-9-yl)-4,6-dicyanobenzene (4CzIPN) in photocatalytic transformations. *Chem. Commun.* **55**, 5408-5419, (2019).
[18] Vega-Peñaloza, A., Mateos, J., Companyó, X., Escudero-Casao, M. & Dell'Amico, L. A Rational Approach to Organo-Photocatalysis: Novel Designs and Structure-Property Relationships. *Angew. Chem., Int. Ed.* **133**, 1096–1111 (2021).

[19] Tlili, A. & Lakhdar, S. Acridinium Salts and Cyanoarenes as Powerful Photocatalysts: Opportunities in Organic Synthesis. *Angew. Chem., Int. Ed.* 19526–19549 (2021).
[20] Bortolato, T., Cuadros, S., Simionato, G. & Dell'Amico, L. The advent and development of organophotoredox catalysis. *Chem. Commun.* **58**, 1263–1283 (2022).
[21] Luo, J. & Zhang, J. Donor–Acceptor Fluorophores for Visible-Light-Promoted Organic Synthesis: Photoredox/Ni Dual Catalytic C(sp3)–C(sp2) Cross-Coupling. *ACS Catal.* **6**, 873–877 (2016).
[22] Zhu, Z. *et al.* Cell-Penetrating Peptides Transport Noncovalently Linked Thermally Activated Delayed Fluorescence Nanoparticles for Time-Resolved Luminescence Imaging. *J. Am. Chem. Soc.* **140**, 17484-17491, (2018).
[23] Donabauer, K. *et al.* Photocatalytic carbanion generation – benzylation of aliphatic aldehydes to secondary alcohols. *Chem. Sci.* **10**, 5162-5166, (2019).
[24] Grotjahn, S. & König, B. Photosubstitution in Dicyanobenzene-based Photocatalysts. *Org. Lett.* **23**, 3146-3150, (2021).
[25] Kong, D. *et al.* Fast Carbon Isotope Exchange of Carboxylic Acids Enabled by Organic Photoredox Catalysis. *J. Am. Chem. Soc.* **143**, 2200-2206, (2021).
[26] Babin, V. *et al.* Photochemical Strategy for Carbon Isotope Exchange with CO2. *ACS Catal.* **11**, 2968-2976, (2021).
[27] Garreau, M., Le Vaillant, F. & Waser, J. C-Terminal Bioconjugation of Peptides through Photoredox Catalyzed Decarboxylative Alkynylation. *Angew. Chem., Int. Ed.* **58**, 8182-8186, (2019).
[28] Liu, X.-Y., Ji, X., Heinis, C. & Waser, J. Peptide-Hypervalent Iodine Reagent Chimeras: Enabling Peptide Functionalization and Macrocyclization. *Angew. Chem., Int. Ed.* **62**, e202306036, (2023).
[29] Thiruvengadam, M., Venkidasamy, B., Thirupathi, P., Chung, I.-M. & Subramanian, U. β-Casomorphin: A complete health perspective. *Food Chem.* **337**, 127765, (2021).
[30] Del Gatto, A., De Simone, M., de Paola, I., Saviano, M. & Zaccaro, L. Investigation of the Best Conditions to Obtain c(RGDfK) Peptide on Solid Phase. *Int. J. Pept. Res. Ther.* **17**, 39-45, (2011).
[31] Jones, R. E., Bourdette, D., Offner, H. & Vandenbark, A. A. The synthetic 87–99 peptide of myelin basic protein is encephalitogenic in Buffalo rats. *J. Neuroimmunol.* **37**, 203-212, (1992).
[32] Webb, M. L., Taylor, D. S. & Molloy, C. J. Effects of thrombin receptor activating peptide on phosphoinositide hydrolysis and protein kinase C activation in cultured rat aortic smooth muscle cells: evidence for "tethered-ligand" activation of smooth muscle cell thrombin receptors. *Biochem. Pharmacol.* **45**, 1577-1582, (1993).
[33] Puleo, D. A. & Bizios, R. RGDS tetrapeptide binds to osteoblasts and inhibits fibronectin-mediated adhesion. *Bone* **12**, 271-276, (1991).
[34] Gomez, J. A. *et al.* Cell-Penetrating Penta-Peptides (CPP5s): Measurement of Cell Entry and Protein-Transduction Activity. *Pharmaceuticals* **3**, 3594-3613, (2010).
[35] Lin, Y.-Z., Yao, S., Veach, R. A., Torgerson, T. R. & Hawiger, J. Inhibition of Nuclear Translocation of Transcription Factor by a Synthetic Peptide Containing a Cell Membrane-permeable Motif and Nuclear Localization Sequence. *J. Biol. Chem.* **270**, 14255-14258, (1995).
[36] Wojciechowska, M., Miszkiewicz, J. & Trylska, J. Conformational Changes of Anoplin, W-MreB1–9, and (KFF)3K Peptides near the Membranes. *Int. J. Mol. Sci.* **21**, 9672, (2020).
[37] Speckmeier, E., Fischer, T. G. & Zeitler, K. A Toolbox Approach To Construct Broadly Applicable Metal-Free Catalysts for Photoredox Chemistry: Deliberate Tuning of Redox Potentials and Importance of Halogens in Donor–Acceptor Cyanoarenes. *J. Am. Chem. Soc.* **140**, 15353-15365, (2018).
[38] Feuillastre, S. *et al.* Design and Synthesis of New Circularly Polarized Thermally Activated Delayed Fluorescence Emitters. *J. Am. Chem. Soc.* **138**, 3990-3993, (2016).
[39] Etherington, M. K. *et al.* Persistent Dimer Emission in Thermally Activated Delayed Fluorescence Materials. *J. Phys. Chem. C.* **123**, 11109-11117, (2019).
[40] Koren, E., Apte, A., Sawant, R. R., Grunwald, J. & Torchilin, V. P. Cell-penetrating TAT peptide in drug delivery systems: Proteolytic stability requirements. *Drug Delivery* **18**, 377-384, (2011).
[41] Kim, S., Nam, H. Y., Lee, J. & Seo, J. Mitochondrion-Targeting Peptides and Peptidomimetics: Recent Progress and Design Principles. *Biochemistry* **59**, 270-284, (2020).
[42] Kalderon, D., Roberts, B. L., Richardson, W. D. & Smith, A. E. A short amino acid sequence able to specify nuclear location. *Cell* **39**, 499-509, (1984).
[43] Grossmann, T. N. *et al.* Inhibition of oncogenic Wnt signaling through direct targeting of β-catenin. *Proc. Natl. Acad. Sci.* U. S. A **109**, 17942-17947, (2012).

[44] Diderich, P. *et al.* Phage Selection of Chemically Stabilized α-Helical Peptide Ligands. *ACS Chem. Biol.* **11**, 1422-1427, (2016).
[45] Yurash, B. *et al.* Photoluminescence Quenching Probes Spin Conversion and Exciton Dynamics in Thermally Activated Delayed Fluorescence Materials. *Adv. Mater* **31**, 1804490 (2019).
[46] Reichardt, C. Solvatochromic Dyes as Solvent Polarity Indicators. *Chem. Rev.* **94**, 2319–2358 (1994).
[47] Tyson, E. L., Ament, M. S. & Yoon, T. P. Transition Metal Photoredox Catalysis of Radical Thiol-Ene Reactions. *J. Org. Chem.* **78**, 2046-2050, (2013).
[48] Choi, H., Kim, M., Jang, J. & Hong, S. Visible-Light-Induced Cysteine-Specific Bioconjugation: Biocompatible Thiol–Ene Click Chemistry. *Angew. Chem., Int. Ed.* **59**, 22514-22522, (2020).
[49] Buksh, B. F. *et al.* μMap-Red: Proximity Labeling by Red Light Photocatalysis. *J. Am. Chem. Soc.* **144**, 6154-6162, (2022).
[50] Oakley, J. V. *et al.* Radius measurement via super-resolution microscopy enables the development of a variable radii proximity labeling platform. *Proc. Natl. Acad. Sci.* U. S. A **119**, e2203027119, (2022).
[51] Tay, N. E. S. *et al.* Targeted activation in localized protein environments via deep red photoredox catalysis. *Nat. Chem.* **15**, 101-109, (2023).
[52] Gu, Y. *et al.* The challenges and opportunities of αvβ3-based therapeutics in cancer: From bench to clinical trials. *Pharmacol. Res.* **189**, 106694 (2023).
[53] Liu, Z., Wang, F. & Chen, X. Integrin αvβ3-targeted cancer therapy. *Drug Dev. Res.* **69**, 329–339 (2008).